micro

MDPI

Article

Preparation and Characterization of Tiamulin-Loaded Niosomes for Oral Bioavailability Enhancement in *Mycoplasma*-Infected Broilers

Shimaa G. Abonashey [1], Amr Gamal Fouad [2], Hatem A. F. M. Hassan [3,4], Ahmed H. El-Banna [5], Mostafa A. Shalaby [6], Elham Mobarez [1], Sherif Ashraf Fahmy [7,*] and Hossny A. El-Banna [6,*]

1 Department of Biochemistry, Animal Research Institute, Dokki, Giza 12618, Egypt
2 Department of Pharmaceutics and Industrial Pharmacy, Faculty of Pharmacy, Beni-Suef University, Beni Suef 62511, Egypt
3 Medway School of Pharmacy, University of Kent, Central Avenue, Chatham Maritime, Canterbury ME4 4TB, UK
4 Department of Pharmaceutics and Industrial Pharmacy, Faculty of Pharmacy, Cairo University, Cairo 11562, Egypt
5 Michael Sayegh Faculty of Pharmacy, Aqaba University of Technology, Aqaba, Jordan
6 Pharmacology Department, Faculty of Veterinary Medicine, Cairo University, Cairo 12211, Egypt
7 Department of Pharmaceutics and Biopharmaceutics, University of Marburg, Robert-Koch-Str. 4, 35037 Marburg, Germany
* Correspondence: sheriffahmy@aucegypt.edu (S.A.F.); drelbanna3@cu.edu.eg (H.A.E.-B.)

Abstract: *Mycoplasma* infections pose significant challenges in the poultry industry, necessitating effective therapeutic interventions. Tiamulin, a veterinary antibiotic, has demonstrated efficacy against *Mycoplasma* species. However, the emergence of resistant *Mycoplasma* species could dramatically reduce the therapeutic potential, contributing to economic losses. Optimizing the tiamulin's pharmacokinetic profile via nanocarrier incorporation could enhance its therapeutic potential and reduce the administration frequency, ultimately reducing the resistant strain emergence. Niosomes, a type of self-assembled non-ionic surfactant-based nanocarrier, have emerged as a promising drug delivery system, offering improved drug stability, sustained release, and enhanced bioavailability. In this study, niosomal nanocarriers encapsulating tiamulin were prepared, characterized and assessed in *Mycoplasma*-inoculated broilers following oral administration. Differential scanning colorimetry (DSC) confirmed the alterations in the crystalline state following components integration into the self-assembled structures formed during the formulation procedure. Transmission electron microscopy (TEM) showed the spherical nanostructure of the formed niosomes. The formulated nanocarriers exhibited a zeta potential and average hydrodynamic diameter of -10.65 ± 1.37 mV and 339.67 ± 30.88 nm, respectively. Assessment of the pharmacokinetic parameters following oral administration to *Mycoplasma gallisepticum*-infected broilers revealed the ability of the niosomal nanocarriers to increase the tiamulin's bioavailability and systemic exposure, marked by significantly higher area under the curve (AUC) ($p < 0.01$) and prolonged elimination half-life ($T_{1/2}$) ($p < 0.05$). Enhanced bioavailability and prolonged residence time are crucial factors in maintaining therapeutic concentrations at reduced doses and administration frequencies. This approach provides a viable strategy to decrease the risk of subtherapeutic levels, thereby mitigating the development of antibiotic resistance. The findings presented herein offer a sustainable approach for the efficient use of antibiotics in veterinary medicine.

Keywords: tiamulin; niosomes; *Mycoplasma gallisepticum*; oral administration; oral bioavailability

Citation: Abonashey, S.G.; Fouad, A.G.; Hassan, H.A.F.M.; El-Banna, A.H.; Shalaby, M.A.; Mobarez, E.; Fahmy, S.A.; El-Banna, H.A. Preparation and Characterization of Tiamulin-Loaded Niosomes for Oral Bioavailability Enhancement in *Mycoplasma*-Infected Broilers. *Micro* **2024**, *4*, 734–750. https://doi.org/10.3390/micro4040045

Academic Editor: Laura Chronopoulou

Received: 16 October 2024
Revised: 20 November 2024
Accepted: 23 November 2024
Published: 27 November 2024

1. Introduction

Mycoplasma gallisepticum stands out as one of the most formidable causative agent of chronic respiratory disease in chickens, significantly affecting the poultry industry. The

prevailing strategy for controlling *Mycoplasma* infections involves the use of antimicrobial agents. Tiamulin is a semisynthetic antibiotic derived from pleuromutilin that originates from the tricyclic diterpenoid pleuromutilin found in the fungus *Pleurotus mutilus*. As an efficient antimycoplasmal drug extensively utilized in veterinary medicine, tiamulin exerts its activity by hindering bacterial protein synthesis, specifically by binding to the 50S ribosomal subunit. Nevertheless, the swift rise of antibiotic-resistant *Mycoplasma* strains, as reported in recent studies, undermines the remarkable benefits that can be attained through the use of tiamulin [1–4]. This is further exacerbated by the emergence of multiple drug resistance and the alarming risk posed by the outbreak of untreatable infections with *Mycoplasma* [5].

Frequent and prolonged exposure of bacterial populations to antibiotics creates a selective pressure favoring the survival and proliferation of resistant strains [6]. Consequently, the reduced exposure of *Mycoplasma* populations to tiamulin can impede the development of resistance by minimizing the opportunities for genetic mutations or adaptations that confer antibiotic resistance [7]. Reducing the administration frequency of antibiotics is a crucial approach in combatting resistance development [8]. In addition, augmenting the bioavailability of antibiotics at reduced doses represents another pivotal strategy to mitigate resistance development. The improved bioavailability can facilitate the achievement of therapeutic concentrations with lower overall doses, minimizing the selective pressure on bacteria to evolve resistance [9]

Addressing the pressing issue of antibiotic resistance necessitates innovative approaches to enhance the precision and efficacy of antibiotic delivery. One promising avenue is the utilization of advanced drug delivery mechanisms, with nanoparticles emerging as a focal point in recent research [10–12]. Nanoscopic materials have shown the ability to improve the effectiveness of loaded therapeutic cargo [13–20]. Additionally, nanoparticles previously demonstrated their efficacy as carriers for antibiotics such as tobramycin, cephalexin, and ciprofloxacin [21–23]. Niosomes are nano-sized carriers consisting of bilayers formed by self-assembled non-ionic surfactants, typically stabilized through the incorporation of cholesterol [24–26]. Featured by their biodegradability, biocompatibility, and chemical stability, niosomes have been widely employed to enhance drug bioavailability [24,27–29]. The combination of reduced administration frequency and enhanced bioavailability, facilitated by innovative drug delivery systems such as niosomes, holds significant promise for addressing the challenge of antibiotic resistance developed by *Mycoplasma* infections [30]. This approach not only seeks to preserve the effectiveness of tiamulin but also aligns with the broader goal of responsible antibiotic use in safeguarding the long-term viability of antimicrobial therapies in the poultry industry.

We previously demonstrated niosomes' ability to improve the bioavailability of florfenicol, a veterinary antibiotic, through the oral administration route [31]. Employing a non-invasive administration approach for delivering niosomes to chickens presents substantial advantages over more invasive methods, particularly parenteral administration. This approach prioritizes animal welfare by minimizing stress and discomfort, crucial for maintaining the overall health of the birds. Furthermore, the practicality and ease of non-invasive methods, such as oral administration, make them well suited for large-scale implementation in the poultry industry, streamlining processes and reducing labor intensity. The reduced risk of infection and tissue damage associated with non-invasive routes adds another layer of benefit, contributing to the birds' health and productivity. The reduced complexity and enhanced compliance associated with non-invasive approaches render them an attractive choice for the seamless incorporation of cutting-edge drug delivery systems into poultry health management practices.

As such, exploring the potential of niosomes as a tiamulin delivery nanocarrier holds promise for overcoming the emerging antibiotic-resistant *Mycoplasma* strains. Accordingly, we proposed that the niosomes' formulation capacity to improve tiamulin's bioavailability and reduce administration frequency could address the growing challenge of antibiotic resistance in *Mycoplasma* strains, thereby contributing to the sustainability of antimicrobial

therapies in the poultry industry. To this end, we developed and characterized a tiamulin-loaded niosomal formulation. Additionally, we assessed pharmacokinetics following oral administration to *Mycoplasma*-infected chickens. Furthermore, we evaluated oral bioavailability in healthy broilers to deepen our understanding of the nano-formulation's pharmacokinetic profile in the presence of *Mycoplasma* infection.

2. Materials and Methods

2.1. Materials

Tiamulin hydrogen fumarate powder with purity ≥98.0% was obtained from Pharma-Swede (Cairo, Egypt). Cholesterol, DDP, Tween 60, and Span 60 were purchased from Sigma Aldrich (Burlington, MA, USA). Methanol and chloroform were purchased from Corner-Lab Company (Cairo, Egypt). *Mycoplasma gallisepticum* (*MG*) *S 6 strain* (ATCC 19610) was obtained from the Microbiological Resources Centre (Mircen, Cairo, Egypt). *Mycoplasma gallisepticum* field isolate strain (EIS-C3-09) was obtained from the *Mycoplasma* department of the Animal Health Research Institute (Giza, Egypt). Nylon filter (0.45 µm) was purchased from Millipore (Burlington, MA, USA).

2.2. Preparation of Tiamulin-Loaded Niosomes (TLN)

Tiamulin-loaded niosomes were formulated using the thin film hydration method [32]. In a round flask, tiamulin (1 mg), along with 30 mg of Span 60 and cholesterol in a molar ratio of 1:1, was dissolved in a chloroform and methanol mixture. The combined solution was subsequently rotary-evaporated under reduced pressure at 40 °C until a thin film was formed. The resulting dried thin layer was then hydrated with 10 mL of phosphate buffer of pH 7.4 at 60 °C for 2 h. The formulated mixture underwent sonication for 30 min and was subsequently centrifuged using a cooling centrifuge at a speed of 15,000 rpm and 4 °C for 1 h, facilitating the separation of the entrapped drug from the unentrapped one. The collected niosomal pellets were re-suspended in phosphate buffer, and the prepared formulation was stored at 4 °C for subsequent studies.

2.3. Characterization of TLN

2.3.1. Transmission Electron Microscopy (TEM)

The morphological features of the TLN formulation were determined using TEM (Carl Zeiss, Oberkochen, Germany) [33]. The freshly prepared sample was deposited onto the surface of a carbon-coated copper grid and stained with a drop of a 1% aqueous solution of phosphotungstic acid dye to enhance visualization during TEM analysis.

2.3.2. Particle Size, Size Distribution, and Zeta Potential

The prepared niosome formulation's particle size, poly dispersity index (PDI), and zeta potential were determined using the Malvern PCS4700 Instrument (Malvern Instruments, Malvern, UK) [33,34]. TLN samples were appropriately diluted with de-ionized water prior to measurements. Three independent measurements were conducted at room temperature.

2.3.3. Differential Scanning Calorimetry (DSC)

The thermal behavior of TLN and its contained ingredients, tiamulin, Span 60, and cholesterol, was determined using a DSC analyzer (60F3, NETZSCH-Geratebau GmbH, Maia, Germany) equipped with a liquid nitrogen cooling system [35]. The analysis was performed with a heating rate of 5 °C/min under a nitrogen gas flow of 25 mL/min, and the temperature ranged from room temperature to 200 °C. An empty aluminum pan was used as a reference.

2.3.4. Entrapment Efficiency (EE%)

The TLN suspension was centrifuged at 15,000 rpm for 2 h at a temperature of 4 °C to separate the entrapped tiamulin. Methanol was used to dissolve the entrapped tiamulin. Tiamulin quantification was carried out utilizing high-performance liquid chromatography (HPLC).

Tiamulin was separated isocratically using a C18 analytical column (150 mm × 4.6 mm) at a maximum wavelength of 212 nm. The mobile phase consisted of a 40:60 *v*/*v* of 1% ammonium carbonate and acetonitrile, delivered at a flow rate of 1 mL per minute with injection volumes of 20 µL [36]. The EE% was determined using the following equation [37].:

$$\%EE = \frac{E_t}{E_i} \times 100 \quad (1)$$

where E_t is the amount of entrapped tiamulin and E_i is the initial tiamulin amount.

2.3.5. In Vitro Release

The release profile of tiamulin in its solution and niosome-loaded forms was evaluated utilizing a Hanson dissolution apparatus [38]. To a dialysis bag, 2 mg of free or niosome-loaded tiamulin were transferred. The dialysis bag was subsequently submerged in 25 mL of phosphate buffer (pH 7.4) that was used as the release medium. The Hanson dissolution apparatus (USA) was set to operate at 100 rpm and maintained at a temperature of 37 ± 0.5 °C. At specified intervals, 2 mL samples were withdrawn from each receptor compartment and replaced with an equivalent volume of fresh medium. The released tiamulin was quantified using HPLC and the percentage release was determined using the following equation in triplicate:

$$\%Release = \frac{R_t}{R_i} \times 100 \quad (2)$$

where R_t is the amount of tiamulin released at time t and R_i is the initial amount of entrapped tiamulin.

2.4. Determination of Mycoplasma gallisepticum Strain Sensitivity

2.4.1. *Mycoplasma gallisepticum* Strain

Mycoplasma gallisepticum field isolate strain (EIS-C3-09), sourced from the *Mycoplasma* Department at the Animal Health Research Institute in Dokki, Giza, Egypt, was utilized in experimental infection. To enhance the virulence of this strain, it underwent a passage through the yolk sacs of specific pyrogen-free eggs. Subsequently, the yolk and allantoic fluid were collected and utilized for the inoculation process [39]. Following the enhancement in virulence, an in vitro assessment was carried out to determine the strain's sensitivity to the antimycoplasmal drug, utilizing the minimum inhibitory concentration (MIC) method.

2.4.2. The Growth Media

The growth medium employed for the sensitivity test was fortified with 12% inactivated horse serum [40]. The broth utilized for culture propagation underwent sterilization through filtration using a Millipore filter equipped with a 0.2 µm cellulose membrane. Subsequently, the agar medium was prepared by subjecting the medium to autoclaving at 121 °C for 20 min, with the addition of 1.5% agar. Following autoclaving, cysteine, penicillin, thallium acetate, and swine serum were aseptically introduced into the medium and stored at 4 °C.

2.4.3. Determination of Minimum Inhibitory Concentration (MIC) Against Mycoplasma

The determination of the minimum inhibitory concentration (MIC) of tiamulin against both the *Mycoplasma gallisepticum* (*MG*) *S 6 strain* (ATCC 19610) and the field isolate strain (EIS-C3-09) was conducted through a modified MIC assay method [41]. A *Mycoplasma gallisepticum* titer of 10^7 CFU/mL in the *Mycoplasma* medium was prepared. Serial two-fold dilutions of tiamulin were then prepared within the concentration range of 0.0156–32 µg/mL, utilizing MG culture medium as the diluent (at a 1:1 dilution). All experimental procedures were meticulously performed in triplicate. The MIC was defined

as the lowest concentration of tiamulin at which no discernible change in the color of the culture medium was observed.

2.5. In Vivo Studies

2.5.1. Experimental Birds

The Institutional Animal Care and Use Committee (IACUC) at the Faculty of Veterinary Medicine, Cairo University, Egypt approved the animal use protocol (Vet CU 09092023749). The experiments involving animal use were conducted in accordance with the guidelines and regulations of the IACUC at the Faculty of Veterinary Medicine, Cairo University, Egypt.

Clinically healthy, one-week-old, Hubbard chickens, verified as *Mycoplasma gallisepticum*-free, were procured from Elarabia Poultry Breeding Farm. These chicks were nourished with antibiotic- and anticoccidial-free poultry ration (ad libitum), accompanied by unrestricted access to water for a period of two weeks. This dietary regimen was implemented to facilitate the full elimination of antibacterial agents from the body. Chickens were housed in an environment characterized by a constant temperature, relative humidity ranging from 45% to 65%, and a 12 h lighting cycle. Prior to drug administration, the birds underwent an overnight fasting period.

2.5.2. Induction of *Mycoplasma gallisepticum* Intratracheal Infection

At three weeks of age, chickens free from *Mycoplasma gallisepticum* underwent thorough screening by collecting tracheal swabs for molecular detection using polymerase chain reaction (PCR) to confirm their negative status for *Mycoplasma gallisepticum*. Subsequently, these chickens were subjected to inoculation via the intraocular/intranasal route with 0.1 mL containing 107 colony-forming units (CFU) of MG culture. An additional inoculum of 0.1 mL was administered via the intratracheal route [42]. The chickens were observed for 6–21 days till the appearance of the clinical signs [43]. The confirmation of infection was established through the observation of clinical manifestations and the serum plate agglutination test (SPA). The experiments were conducted under conditions adhering to the institutional biosafety guidelines.

2.5.3. Serum Plate Agglutination

A single volume, approximately 0.02 mL, of serum was dispensed onto a pristine white glass plate, followed by an equal volume of stained MG antigen. Subsequently, a stirring rod was employed to evenly distribute the mixture over a circular area of approximately 1.5 cm in diameter. The plate was gently rocked for a duration of 2 min. The occurrence of agglutination was evidenced by the flocculation of the antigen within this 2 min timeframe [44]. The test encompassed both known positive and negative controls, and retests involved serial dilutions of any sera exhibiting agglutination after undergoing heating at 56 °C for 30 min. Sera that maintained strong reactivity even after dilution (1/4 or more) were considered positive.

2.5.4. Serum Plate Agglutination (SPA) Test

On a glass plate, 0.03 mL of antigen was dispensed along with an equivalent volume of fresh serum using a pipette [45]. The contents underwent thorough mixing by stirring with a glass rod, followed by gentle rocking. The interpretation of results took place within a 2 min timeframe. Positive cases revealed a gradual formation of granules, discernible during the rocking motion. Conversely, negative cases displayed the absence of such granular formations. A meticulous record was maintained for all serum plate agglutination (SPA) outcomes. It is noteworthy that in our study, the SPA test employed a crystal violet-stained *Mycoplasma gallisepticum* commercial antigen procured from Intervet Company Ltd. (Boxmeer, The Netherlands).

2.5.5. Oral Administration of Free Tiamulin or TLN to *Mycoplasma gallisepticum*-Infected Broilers

Broiler chickens that were experimentally infected with avian pathogenic *Mycoplasma* gallisepticum (MG) were randomly segregated into two subgroups, each comprising six individuals (n = 6). A single dose of 30 mg/kg body weight of free or noisome-contained tiamulin was administered through the oral route to the first or second subgroups, respectively [46,47].

2.5.6. Oral Administration of Free Tiamulin or TLN to Clinically Healthy Broilers

Clinically healthy chickens were randomly distributed into two subgroups; each subgroup contained six individuals (n = 6). A single dose of free or noisome-contained tiamulin was orally administered at 30 mg/kg body weight to the first or second subgroups in this healthy cohort, respectively.

2.5.7. Determination of Tiamulin Concentration in Plasma

Blood samples (0.75–1 mL) were collected from all avian subjects through the median tarsometatarsal vein into heparinized tubes at specific timepoints post-administration. Subsequently, all collected samples underwent centrifugation at 1800× *g* for 10 min. The resulting clear plasma was carefully transferred to Eppendorf tubes and promptly frozen at –80 °C until the time of assay. The quantification of tiamulin in plasma was conducted using LC-MS, following established protocols with slight adjustments [48]. Chromatographic separation of tiamulin was achieved utilizing a C18 column (Luna, 150 mm × 2 mm, I.D, 5 µm) maintained at a temperature of 30 °C. A gradient elution program was employed with eluent A (water containing 0.1% formic acid) and eluent B (methanol containing 0.1% formic acid) at a flow rate of 0.4 mL/min. The elution commenced at 90% eluent A for 7.0 min, followed by a linear decrease to 10% eluent A over 10 min. Subsequently, the system returned to the initial conditions in 0.1 min and was conditioned with 10% solvent A for 0.9 min. The total run time for a sample was 20.0 min, and the injection volume was set at 20 µL. The mass spectrometer was operated in positive ion and multiple reaction monitoring (MRM) mode with precursor to product qualifier transitions m/z 494.500/192.200 and m/z 494.500/119.200. All parameters of the liquid chromatography (LC) and mass spectrometry (MS) were managed through Analyst_1.5 software. The spray voltage was optimized at 4000 V, source temperature at 550 °C, and curtain gas, and auxiliary gas (nitrogen) pressures were set at 25 and 10 psi, respectively. Nitrogen served as the collision gas at a pressure of 40 psi; collision energy (CE) was adjusted to 29 and 55 V, and collision extraction potential (CXP) to 12 V, for transitions 494.500/192.200 and m/z 494.500/119.200, respectively. The dwell time was set at 100 ms. Standard curves were established by spiking tiamulin standards in chicken plasma and tissues within the concentration range of 0.01–10 µg/mL. Chicken plasma samples were allowed to thaw at room temperature. Subsequently, 0.25 mL of plasma samples were subjected to extraction with 0.75 mL of acetonitrile. The resulting mixture was vortexed for 1 min and then centrifuged at 16,000 g for 10 min. The upper organic layer was carefully transferred and filtrated through a 0.22 mm syringe filter, and 20 µL of the filtered solution was injected into the LC-MS/MS system for analysis. The pharmacokinetic parameters were analyzed using Kinetica 2000 (Version 3.0, InnaPhase Corporation, Philadelphia, PA, USA).

2.6. Statistical Analysis

The pharmacokinetic parameters obtained were analyzed with a non-parametric Mann–Whitney test using GraphPad Prism version 7.00 (USA) to determine the differences between the groups.

3. Results and Discussion

3.1. In Vitro Characterization of TLN

Niosomes can be described as self-assembled spherical vesicles formed from non-ionic surfactants, often stabilized with cholesterol to enhance rigidity and prevent leakage of encapsulated ingredients (Figure 1A) [29]. The synthesis of the noisome formulation was achieved using the thin film hydration method, a widely used technique for the preparation of lipid-based delivery systems due to its simplicity and efficiency. This method involves the formation of a surfactant thin film by evaporating an organic solvent mixture, followed by hydration with an aqueous phase to form the self-assembled vesicles [31]. The transmission electron microphotograph of the TLN formulation showed that the nanoparticles exhibited an approximately spherical shape, appearing as discernible black dots without evident aggregation (Figure 1B). The evaluation of vesicle size is crucial in determining the niosomal effectiveness, as a nanocarrier. Smaller vesicles offer a larger surface area that could enhance drug absorption [49–51]. The formulated TLN exhibited a small particle size of 339.67 ± 30.88 nm, suggesting the formation of nano-sized vesicles (Figure 1C). To ascertain the size distribution, and homogeneity of vesicle size within a sample, the PDI was employed [33]. The analysis of the prepared TLN's PDI unveiled a low value of 0.149 ± 0.07, indicating homogeneity and a narrow distribution of particle size. As illustrated in Figure 1D, the formulated TLN exhibited a net mean negative surface charge of −10.65 ± 1.37 mV, indicating electrostatic stabilization of the colloidal dispersion [49].

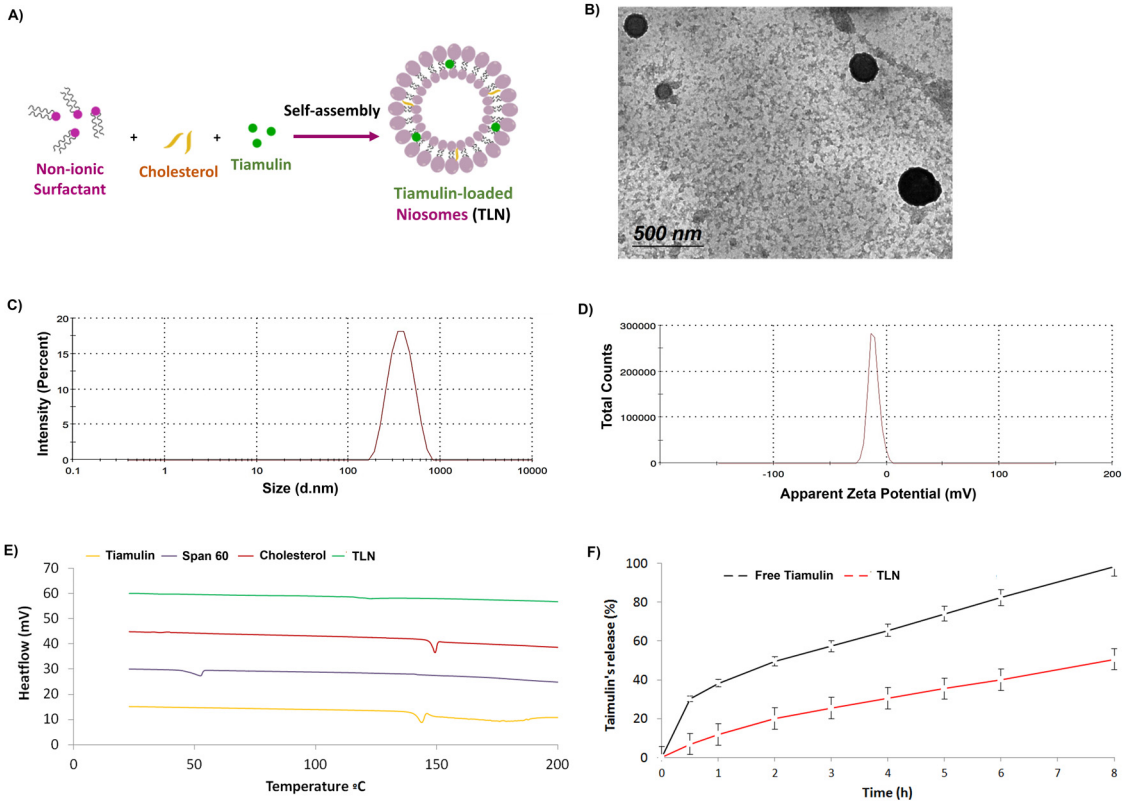

Figure 1. Characterization of TLN. (**A**) Structural components of TLN. (**B**) TLN morphology visualized using TEM. (**C**) Particle size distribution of the TLN formulation. (**D**) Zeta potential of the TLN formulation. (**E**) DSC thermograms of tiamulin, Span 60, cholesterol, and TLN. (**F**) In vitro release profile of tiamulin from the TLN formulation, results represent the mean value ± S.D. (n = 3).

The EE% was determined to evaluate the loading efficiency of the niosomal formulation. The TLN formulation exhibited an EE% of 71.05 ± 0.58%. The intrinsic features of Span 60, encompassing characteristics such as the length of the C-H alkyl chains, a low HLB value, and the presence of a hydrophobic moiety, in conjunction with a high gel-liquid

phase transition temperature and low surface free energy, can facilitate the generation of niosomes with high entrapment efficiency and a small particle size [37,52]. Additionally, niosome integrity, physical stability, and rigidity could be enhanced by the incorporation of cholesterol within the vesicular structure [53–55]. Nevertheless, the increase in the amount of incorporated cholesterol can be accompanied by an increase in the size of the prepared niosomes [35]. Moreover, higher amounts of cholesterol may compete with the drug incorporation within the bilayers leading to a decrease in the entrapment efficiency [56,57]. In our study, the TLN formulation was prepared using 30 mg of Span 60 and cholesterol with a 1:1 molar ratio [37,56,57]. Previous studies reported that increasing the amount of non-ionic surfactants and cholesterol may lead to an increase in the hydrophobic domain volume and the number of niosomes formed [37,58]. This, in turn, could result in an increase in entrapment efficiency and particle size. However, the further increase in the amount of incorporated non-ionic surfactants and cholesterol above 30 mg may lead to a reduction in the entrapment efficiency and larger particle sizes [37,58]. This may be due to the formation of mixed micelles along with the niosomal vesicles. Accordingly, the careful selection of the Span 60 and cholesterol in a 1:1 molar ratio in our study contributed to favorable niosomal characteristics, including a small particle size of 339.67 ± 30.88 nm, homogeneity with a low PDI of 0.149 ± 0.07, and high entrapment efficiency.

The application of DSC allows for the assessment of ingredients' crystallinity [59]. The DSC thermogram of pure tiamulin revealed a clear endothermic peak at 147.79 °C, corresponding to its melting point and indicating its crystalline nature (Figure 1E). In the thermal analysis of the Span 60 surfactant, an endothermic peak was observed at its melting point of 52.09 °C, while cholesterol exhibited a similar endothermic peak at 149 °C. The introduction of tiamulin into the niosomes, as evident in the TLN thermogram, led to a reduction in tiamulin's crystallinity, likely attributed to the incorporation of tiamulin within the surfactant bilayer of the niosomal structure in an amorphous form. The absence of peaks corresponding to Span 60 and cholesterol in the TLN thermogram indicated the loss of their crystalline pattern that could be attributed to their amorphous assembly as a bilayer. Collectively, the DSC analysis highlighted the changes in the key ingredients' crystalline state following their incorporation in the vesicular structures generated during the formulation process.

The release profile of tiamulin from the solution form and niosomal formulation was investigated over an 8 h period using a dialysis bag system (Figure 1F). The tiamulin solution exhibited rapid release, with nearly 30% of the drug released within the first hour, reaching almost 100% by the end of this study. In contrast, TLN demonstrated a significantly slower release, with approximately 10% released in the first hour and around 40% after 8 h. This sustained release profile of TLN was likely attributable to the structural integrity of the niosomes, which could act as a diffusion barrier, effectively modulating the release of the encapsulated tiamulin [29].

3.2. In Vitro Antimicoplasmal Activity

The MIC values of free tiamulin and its niosome-contained form against *MG S 6 strain* (ATCC 19610) and the field isolate strain (EIS-C3-09) were determined (Supplementary Figure S1). The MIC of free tiamulin and its niosome-loaded form against *MG S 6 strain* (ATCC 19610) were both 0.0312 μg/mL ± 0.0 (Table 1). Similarly, the observed MIC values for free tiamulin and its niosome-encapsulated form against the MG field isolate strain (EIS-C3-09) were both 0.0624 μg/mL ± 0.0. These findings suggest that niosomal nanocarriers did not influence the internalization of loaded tiamulin or its interaction with *Mycoplasma gallisepticum*. The comparable MIC values indicated that the efficacy remained consistent, whether tiamulin was used in its free or niosome-incorporated forms.

Table 1. MIC of tiamulin (μg/mL) against *Mycoplasma Gallisepticum*.

	MIC of Tiamulin [1] (μg/mL)	
Bacterial Strain	**Free Tiamulin**	**TLN**
MG S 6 strain (ATCC 1961)	0.0312 ± 0.0	0.0312 ± 0.0
MG field isolate strain (EIS-C3-09)	0.0624 ± 0.0	0.0624 ± 0.0

[1] Results represent the mean value ± SD (n = 3).

3.3. Pharmacokinetic Profile of Orally Administered Niosomal Tiamulin in Mycoplasma-Infected Broilers

To evaluate the niosomal potential to improve the oral bioavailability of the encapsulated drug, we assessed the tiamulin's pharmacokinetic properties after the administration of its free or niosomes-loaded form to *Mycoplasma*-infected broilers via the oral route. The results revealed significant differences in key pharmacokinetic parameters between the administered free and noisome-contained tiamulin (Figure 2). Chicken-derived plasma samples were analyzed by LCMS to determine the levels of tiamulin after oral administration. Using standard tiamulin concentrations that ranged from 0.1 to 40 μg/mL in chicken plasma, the calibration curve created showed linear correlation coefficient higher than 0.997 (Supplementary Figure S2).

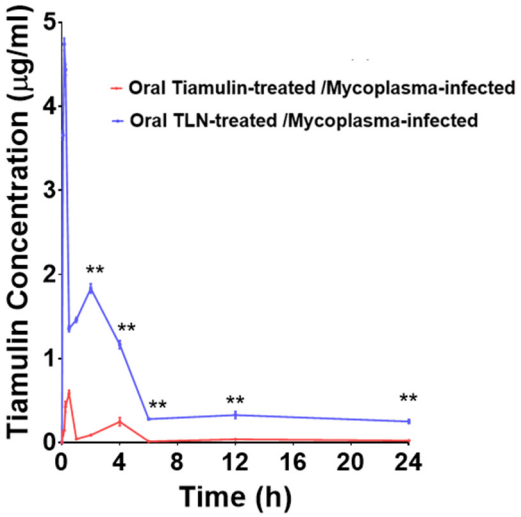

Figure 2. Tiamulin concentration in plasma samples collected from *Mycoplasma*-infected chickens after the administration of free tiamulin or niosome-contained tiamulin at 30 mg /kg body weight. The data presented indicate the average value ± standard deviation (S.D.) (n = 6). ** $p < 0.01$.

The maximum plasma concentration (C_{max}) of tiamulin was markedly higher in *Mycoplasma*-infected broilers receiving niosomal tiamulin than those administered with free tiamulin (Figure 2). This observation suggests that the nanoparticle formulation facilitated more efficient drug absorption. Enhanced drug absorption could be attributed to the nano-formulation's capacity to improve the solubility and permeability of the incorporated tiamulin across biological barriers, such as the intestinal epithelium. Previous studies reported the niosomal ability to increase the loaded drug absorption after oral intake [60,61]. Furthermore, it was previously demonstrated that the surfactant constituents within the niosomal formulations could also potentially inhibit the efflux facilitated by P-glycoprotein (P-gp), a transmembrane efflux protein pump found in the gastrointestinal tract that pumps the drug out of the enterocytes back into the intestinal lumen [61,62]. It could be suggested that the suppressive impact of non-ionic surfactants on P-gp are thought to stem from their capacity to alter membrane fluidity [63]. Consequently, a reduction in P-gp activity could

result in increased drug absorption and higher concentrations in the bloodstream, leading to improved bioavailability.

The mean residence time (MRT) of tiamulin was significantly prolonged in *Mycoplasma*-infected broilers that were treated with TLN (Figure 3). This prolonged exposure could be advantageous in preventing infections or maintaining therapeutic levels over an extended period, potentially reducing the frequency of drug administration. This finding could suggest the niosomes' ability to sustain the incorporated tiamulin release and extend its retention within the body [31]. The elimination $T_{1/2}$ of tiamulin was substantially longer in the oral TLN-administered group, indicating a slower drug elimination process. The prolonged $T_{1/2}$ could indicate that the formulated niosomes may have protected the loaded tiamulin from rapid metabolism or degradation [62,64]. Niosomes could act as drug reservoirs that release the contained tiamulin gradually over time, ultimately leading to prolonged presence of the administered drug. Additionally, niosomal encapsulation could protect tiamulin from enzymatic degradation in the gut, which could allow for reduced drug metabolism and enhanced systemic exposure [65]. The $AUC_{(0-\infty)}$ was significantly higher in the *Mycoplasma*-infected broilers that received oral TLN (Figure 3). This observation reflects an overall increase in the drug exposure, potentially leading to higher bioavailability and a more pronounced therapeutic effect [66].

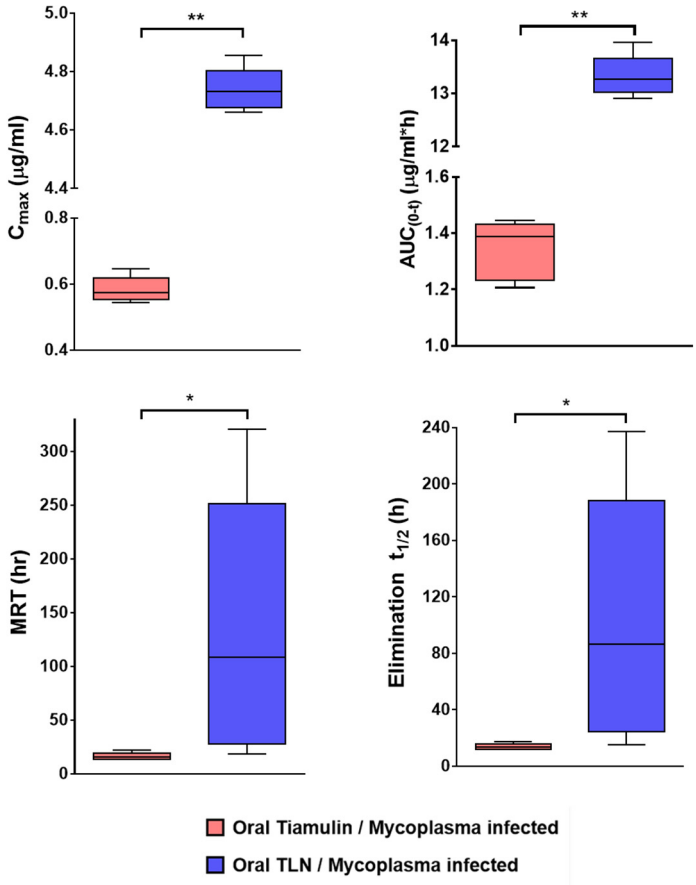

Figure 3. Box plot of C_{max}, $AUC_{(0-\infty)}$ and elimination $T_{1/2}$ of free or niosome-contained tiamulin following the oral administration to *Mycoplasma*-infected broilers. The median value is represented by the horizontal line inside the box, and the whiskers extend to the 10th and 90th percentiles below and above the box, respectively. A Mann–Whitney test was used for statistical analysis. * $p < 0.05$, ** $p < 0.01$.

These findings highlight the potential of niosomal nanoparticle-based drug delivery systems for optimizing the therapeutic effectiveness of tiamulin in *Mycoplasma* infections and may have broader implications for drug delivery strategies in various medical contexts.

Further investigations are warranted to elucidate the precise mechanisms behind these observed enhancements and to validate their applicability in clinical settings.

3.4. Effect of Mycoplasma Infection on the Absorption and Elimination of Orally Administered Niosomal Tiamulin

To address the effect of *Mycoplasma* infection on the pharmacokinetic profiles of noisome-delivered tiamulin after oral administration, the pharmacokinetic parameters were assessed in healthy chickens after oral intake of the free tiamulin or in its noisome-loaded form (Figure 4).

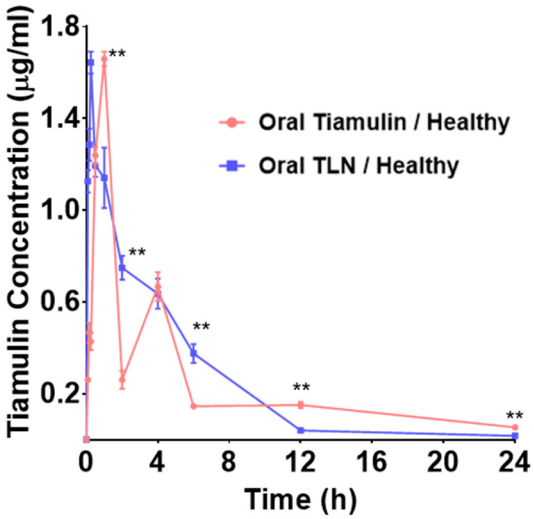

Figure 4. Concentration of tiamulin in plasma samples from healthy chickens, measured after they were orally given 30 mg/kg of either free tiamulin or tiamulin-incorporated in niosomes. The data shown indicate the average ± S.D (n = 6). ** $p < 0.01$.

The C_{max} of tiamulin in healthy broilers orally administered with tiamulin-loaded niosomal nanoparticles was found to be similar to that in broilers receiving free tiamulin, suggesting comparable initial drug exposure (Figure 5). The comparable C_{max} values between the two formulations in healthy broilers suggest that niosomal nanoparticles did not significantly affect the initial drug absorption or peak plasma concentration of tiamulin in healthy broilers. This implies that in healthy conditions, both forms of the drug can initially achieve similar levels in the bloodstream upon oral administration. Conversely, the plasma $AUC_{0-\infty}$ of tiamulin was significantly higher ($p < 0.05$) in healthy broilers treated with niosomal nanoparticles, indicating a more extensive overall drug exposure (Figure 5). Interestingly, a four-fold increase in C_{max} of tiamulin was detected in *Mycoplasma*-infected broilers compared to healthy broilers following oral administration of TLN. This could be attributed to the presence of *Mycoplasma* infections that might alter gastrointestinal physiology, permeability and drug absorption, resulting in different C_{max} values [67].

On the other hand, the MRT and elimination $T_{1/2}$ of tiamulin were significantly longer ($p < 0.01$) in healthy broilers receiving free tiamulin than those administered tiamulin-loaded niosomal nanoparticles. The MRT and elimination $T_{1/2}$ of tiamulin were significantly longer (1.7-fold) in *Mycoplasma*-infected broilers than healthy broilers after oral administration of free tiamulin. In poultry, as in other species, the primary route of metabolism for orally taken tiamulin is hepatic metabolism [68]. Due to the first-pass effect, orally administered tiamulin may undergo hepatic metabolism, which reduces the intact drug fraction reaching the systemic circulation [69]. The liver capacity to metabolize orally administered drugs can be adversely affected by the inflammation or dysfunction caused by *Mycoplasma* infection [70,71]. Thus, the longer MRT and elimination $T_{1/2}$ detected in *Mycoplasma*-infected broilers than healthy ones could be attributed to *Mycoplasma*-induced liver impairment. The fact that oral administration of tiamulin in the form of a niosomal formulation to healthy

broilers markedly shortened the tiamulin MRT and elimination $T_{1/2}$, which were not observed in *Mycoplasma*-infected broilers, could highlight the significant influence of liver metabolism on the niosomal clearance [61]. Similar to the free drug, orally administered nanoparticles that enter the portal circulation following absorption suffer from the first-pass metabolism [61,72]. The results presented herein suggest the dramatic influence of liver metabolism on the nano-formulation compared to the free drug in healthy broilers that may justify the detected longer free tiamulin persistence in healthy broilers. Future studies should also consider tracking tiamulin metabolites following administration in both free and niosome-incorporated forms to better understand the influence of liver metabolism on the pharmacokinetic profile of the nano-formulation.

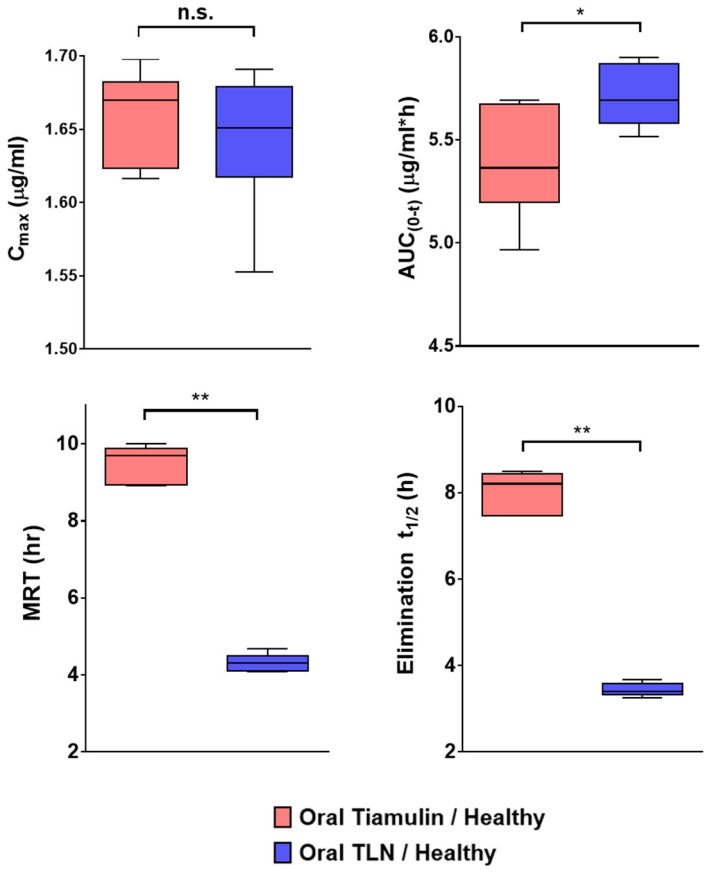

Figure 5. Box plot of C_{max}, $AUC_{(0-\infty)}$, and elimination $T_{1/2}$ of free or niosome-contained tiamulin following the oral administration to healthy broiler. The median value is represented by the horizontal line inside the box, and the whiskers extend to the 10th and 90th percentiles below and above the box, respectively. Mann–Whitney test was used for statistical analysis. * $p < 0.05$, ** $p < 0.01$.

The observed differences in pharmacokinetic parameters between TLN and free tiamulin provide valuable insights into the potential advantages of niosomal nanoparticles as a drug delivery system. While the infected broilers benefited from the extended exposure to tiamulin, healthy broilers primarily exhibited advantages in terms of $AUC_{0-\infty}$ following TLN oral intake. These findings highlight the importance of tailoring drug delivery systems to specific clinical conditions, with niosomal nanoparticles showing promise for optimizing tiamulin therapy in poultry, both in treating infections and potentially in preventive measures for healthy broilers. Further research should delve into the mechanistic aspects of these differences and their clinical implications.

Furthermore, the findings from our study on the pharmacokinetic profile of orally administered niosomal tiamulin in *Mycoplasma*-infected broilers offer strategic opportunities to mitigate the risk of tiamulin resistance. The prolonged MRT and elimination $T_{1/2}$ observed in *Mycoplasma*-infected broilers suggest sustained drug action, providing

a foundation to optimize dosage and administration frequency. By tailoring the dosage regimen based on the sustained release properties of niosomal tiamulin, there is potential to reduce the need for frequent administration, minimizing the risk of subtherapeutic levels that could contribute to resistance. Additionally, the enhanced bioavailability and increased C_{max} support the possibility of maintaining therapeutic levels at lower doses. Considering these advantages, exploring combination therapy with antibiotics having different mechanisms of action becomes a viable strategy, potentially reducing selective pressure and further safeguarding against resistance development.

Our study extensively explored the pharmacokinetic profile of orally administered niosomal tiamulin in healthy and *Mycoplasma*-infected broilers. The higher C_{max} observed in niosomal tiamulin-treated broilers indicated more efficient drug absorption, likely attributed to improved solubility and permeability across biological barriers. The MRT and elimination $T_{1/2}$ further suggest sustained drug release and extended retention. Importantly, the elevated $AUC_{(0-\infty)}$ in *Mycoplasma*-infected broilers receiving oral niosomal tiamulin signifies increased overall drug exposure, enhancing bioavailability and therapeutic efficacy. These findings highlight the potential of niosomal nanoparticles for precise and impactful antibiotic delivery in managing *Mycoplasma* infections in poultry. Considering the convenience of oral administration in poultry farming, our study supports the suitability of the oral route for administering niosomal tiamulin, offering practical and effective drug delivery in the context of poultry health management.

4. Conclusions

Our study encompassed a comprehensive exploration of the pharmacokinetic profile of nanocarrier-loaded tiamulin administered orally to healthy and *Mycoplasma*-infected chickens. The characterization techniques confirmed the nano-sized vesicles' homogeneity, small size, and negative zeta potential, indicative of good stability. DSC further supported the amorphous nature of tiamulin within the niosomal structure. Oral niosomal tiamulin exhibited significant advantages, including higher C_{max} and $AUC_{(0-\infty)}$ as well as prolonged MRT and elimination $T_{1/2}$ in *Mycoplasma*-infected broilers. These findings signify enhanced drug absorption and extended exposure, ultimately leading to improved bioavailability and precise antibiotic delivery in managing *Mycoplasma* infections in poultry. The convenience of oral administration in poultry farming further supports the suitability of this route for niosomal tiamulin, providing a practical and effective drug delivery strategy. Moreover, our study opens up strategic possibilities to address the threat of tiamulin resistance. The heightened bioavailability and protracted residence form the basis for refining dosage schedules and sustaining therapeutic concentrations at reduced doses and administration frequencies. This approach presents a viable means of diminishing the likelihood of subtherapeutic levels that promote resistance development. In essence, our study presents a forward-thinking strategy for promoting sustainable and efficient antibiotic utilization in veterinary medicine. Ongoing research and clinical validation are imperative to translate these promising findings into practical strategies for addressing *Mycoplasma* infections and curtailing antibiotic resistance in poultry.

Supplementary Materials: The following supporting information can be downloaded at: https://www.mdpi.com/article/10.3390/micro4040045/s1, Figure S1: Determination of the minimum inhibitory concentration (MIC) of tiamulin against *Mycoplasma gallisepticum* (MG) strains; Figure S2: Quantification of tiamulin using LC-MS.

Author Contributions: Conceptualization, S.G.A., A.G.F., H.A.F.M.H., A.H.E.-B., M.A.S., E.M., S.A.F. and H.A.E.-B.; methodology, S.G.A., A.G.F., H.A.F.M.H., A.H.E.-B., M.A.S., E.M., S.A.F. and H.A.E.-B.; software, S.G.A., A.G.F., H.A.F.M.H., A.H.E.-B., M.A.S., E.M., S.A.F. and H.A.E.-B.; validation, S.G.A., A.G.F., H.A.F.M.H., A.H.E.-B., M.A.S., E.M., S.A.F. and H.A.E.-B.; formal analysis, S.G.A., A.G.F., H.A.F.M.H., A.H.E.-B., M.A.S., E.M., S.A.F. and H.A.E.-B.; investigation, S.G.A., A.G.F., H.A.F.M.H., A.H.E.-B., M.A.S., E.M., S.A.F. and H.A.E.-B.; resources, S.G.A., A.G.F., H.A.F.M.H., A.H.E.-B., M.A.S., E.M., S.A.F. and H.A.E.-B.; data curation, S.G.A., A.G.F. and M.A.S.; writing—original draft preparation, S.G.A., A.G.F., H.A.F.M.H., A.H.E.-B., M.A.S., E.M., S.A.F. and H.A.E.-B.;

writing—review and editing, S.G.A., A.G.F., H.A.F.M.H., A.H.E.-B., M.A.S., E.M., S.A.F. and H.A.E.-B. All authors have read and agreed to the published version of the manuscript.

Funding: Sherif Ashraf Fahmy acknowledges the financial support and sponsorship received from the Alexander von Humboldt Foundation, Germany.

Institutional Review Board Statement: The animal study protocol was approved by Institutional Animal Care and Use Committee (IACUC) at the Faculty of Veterinary Medicine, Cairo University, Egypt (Vet CU 09092023749).

Informed Consent Statement: Not applicable.

Data Availability Statement: Study data will be made available upon reasonable request.

Conflicts of Interest: The authors declare no conflicts of interest.

References

1. Bottinelli, M.; Gastaldelli, M.; Picchi, M.; Dall'Ora, A.; Borges, L.C.; Ramirez, A.S.; Matucci, A.; Catania, S. The Monitoring of Mycoplasma gallisepticum Minimum Inhibitory Concentrations during the Last Decade (2010–2020) Seems to Reveal a Comeback of Susceptibility to Macrolides, Tiamulin, and Lincomycin. *Antibiotics* **2022**, *11*, 1021. [CrossRef] [PubMed]
2. de Jong, A.; Youala, M.; Klein, U.; El Garch, F.; Simjee, S.; Moyaert, H.; Rose, M.; Gautier-Bouchardon, A.V.; Catania, S.; Ganapathy, K.; et al. Minimal inhibitory concentration of seven antimicrobials to Mycoplasma gallisepticum and Mycoplasma synoviae isolates from six European countries. *Avian Pathol* **2021**, *50*, 161–173. [CrossRef] [PubMed]
3. Beylefeld, A.; Wambulawaye, P.; Bwala, D.G.; Gouws, J.J.; Lukhele, O.M.; Wandrag, D.B.R.; Abolnik, C. Evidence for Multidrug Resistance in Nonpathogenic Mycoplasma Species Isolated from South African Poultry. *Appl. Environ. Microbiol.* **2018**, *84*, e01660-18. [CrossRef] [PubMed]
4. Emam, M.; Hashem, Y.M.; El-Hariri, M.; El-Jakee, J. Detection and antibiotic resistance of Mycoplasma gallisepticum and Mycoplasma synoviae among chicken flocks in Egypt. *Vet. World* **2020**, *13*, 1410–1416. [CrossRef] [PubMed]
5. Pereyre, S.; Tardy, F. Integrating the Human and Animal Sides of Mycoplasmas Resistance to Antimicrobials. *Antibiotics* **2021**, *10*, 1216. [CrossRef]
6. Wiuff, C.; Zappala, R.M.; Regoes, R.R.; Garner, K.N.; Baquero, F.; Levin, B.R. Phenotypic tolerance: Antibiotic enrichment of noninherited resistance in bacterial populations. *Antimicrob. Agents Chemother.* **2005**, *49*, 1483–1494. [CrossRef]
7. Fridman, O.; Goldberg, A.; Ronin, I.; Shoresh, N.; Balaban, N.Q. Optimization of lag time underlies antibiotic tolerance in evolved bacterial populations. *Nature* **2014**, *513*, 418–421. [CrossRef]
8. van Staa, T.P.; Palin, V.; Li, Y.; Welfare, W.; Felton, T.W.; Dark, P.; Ashcroft, D.M. The effectiveness of frequent antibiotic use in reducing the risk of infection-related hospital admissions: Results from two large population-based cohorts. *BMC Med.* **2020**, *18*, 40. [CrossRef]
9. Abreu, R.; Semedo-Lemsaddek, T.; Cunha, E.; Tavares, L.; Oliveira, M. Antimicrobial Drug Resistance in Poultry Production: Current Status and Innovative Strategies for Bacterial Control. *Microorganisms* **2023**, *11*, 953. [CrossRef]
10. Pinto-Alphandary, H.; Andremont, A.; Couvreur, P. Targeted delivery of antibiotics using liposomes and nanoparticles: Research and applications. *Int. J. Antimicrob. Agents* **2000**, *13*, 155–168. [CrossRef]
11. Rathnayake, K.; Patel, U.; Pham, C.; McAlpin, A.; Budisalich, T.; Jayawardena, S.N. Targeted delivery of antibiotic therapy to inhibit Pseudomonas aeruginosa using lipid-coated mesoporous silica core–shell nanoassembly. *ACS Appl. Bio Mater.* **2020**, *3*, 6708–6721. [CrossRef] [PubMed]
12. Toti, U.S.; Guru, B.R.; Hali, M.; McPharlin, C.M.; Wykes, S.M.; Panyam, J.; Whittum-Hudson, J.A. Targeted delivery of antibiotics to intracellular chlamydial infections using PLGA nanoparticles. *Biomaterials* **2011**, *32*, 6606–6613. [CrossRef] [PubMed]
13. Hassan, H.A.F.M.; Haider, M.; Fahmy, S.A. From antigen uptake to immune modulation: The multifaceted potential of peptide nanofibers as vaccine nanocarriers. *Mater. Adv.* **2024**, *5*, 4112–4130. [CrossRef]
14. Sedky, N.K.; Mahdy, N.K.; Abdel-kader, N.M.; Abdelhady, M.M.M.; Maged, M.; Allam, A.L.; Alfaifi, M.Y.; Shamma, S.N.; Hassan, H.A.F.M.; Fahmy, S.A. Facile sonochemically-assisted bioengineering of titanium dioxide nanoparticles and deciphering their potential in treating breast and lung cancers: Biological, molecular, and computational-based investigations. *RSC Adv.* **2024**, *14*, 8583–8601. [CrossRef]
15. Fahmy, S.A.; Sedky, N.K.; Hassan, H.A.F.M.; Abdel-Kader, N.M.; Mahdy, N.K.; Amin, M.U.; Preis, E.; Bakowsky, U. Synergistic Enhancement of Carboplatin Efficacy through pH-Sensitive Nanoparticles Formulated Using Naturally Derived Boswellia Extract for Colorectal Cancer Therapy. *Pharmaceutics* **2024**, *16*, 1282. [CrossRef]
16. Sedky, N.K.; Abdel-Kader, N.M.; Issa, M.Y.; Abdelhady, M.M.M.; Shamma, S.N.; Bakowsky, U.; Fahmy, S.A. Co-Delivery of Ylang Ylang Oil of Cananga odorata and Oxaliplatin Using Intelligent pH-Sensitive Lipid-Based Nanovesicles for the Effective Treatment of Triple-Negative Breast Cancer. *Int. J. Mol. Sci.* **2023**, *24*, 8392. [CrossRef]
17. Hassan, H.A.F.M.; Sedky, N.K.; Nafie, M.S.; Mahdy, N.K.; Fawzy, I.M.; Fayed, T.W.; Preis, E.; Bakowsky, U.; Fahmy, S.A. Sustainable Nanomedicine: Enhancement of Asplatin's Cytotoxicity In Vitro and In Vivo Using Green-Synthesized Zinc Oxide Nanoparticles Formed via Microwave-Assisted and Gambogic Acid-Mediated Processes. *Molecules* **2024**, *29*, 5327. [CrossRef]

18. Fawzy, M.P.; Hassan, H.A.F.M.; Sedky, N.K.; Nafie, M.S.; Youness, R.A.; Fahmy, S.A. Revolutionizing cancer therapy: Nanoformulation of miRNA-34—Enhancing delivery and efficacy for various cancer immunotherapies: A review. *Nanoscale Adv.* **2024**, *6*, 5220–5257. [CrossRef]
19. Hassan, H.A.F.M.; Smyth, L.; Rubio, N.; Ratnasothy, K.; Wang, J.T.W.; Bansal, S.S.; Summers, H.D.; Diebold, S.S.; Lombardi, G.; Al-Jamal, K.T. Carbon nanotubes' surface chemistry determines their potency as vaccine nanocarriers in vitro and in vivo. *J. Control. Release* **2016**, *225*, 205–216. [CrossRef]
20. Haider, M.; Jagal, J.; Alghamdi, M.A.; Haider, Y.; Hassan, H.A.F.M.; Najm, M.B.; Jayakuma, M.N.; Ezzat, H.; Greish, K. Erlotinib and curcumin-loaded nanoparticles embedded in thermosensitive chitosan hydrogels for enhanced treatment of head and neck cancer. *Int. J. Pharm.* **2024**, *666*, 124825. [CrossRef]
21. Ch, M.H.; Targhi, A.A.; Shamsi, F.; Heidari, F.; Moghadam, Z.S.; Mirzaie, A.; Behdad, R.; Moghtaderi, M.; Akbarzadeh, I. Niosome-encapsulated tobramycin reduced antibiotic resistance and enhanced antibacterial activity against multidrug-resistant clinical strains of Pseudomonas aeruginosa. *J. Biomed. Mater. Res. Part A* **2021**, *109*, 966–980.
22. Mirzaie, A.; Peirovi, N.; Akbarzadeh, I.; Moghtaderi, M.; Heidari, F.; Yeganeh, F.E.; Noorbazargan, H.; Mirzazadeh, S.; Bakhtiari, R. Preparation and optimization of ciprofloxacin encapsulated niosomes: A new approach for enhanced antibacterial activity, biofilm inhibition and reduced antibiotic resistance in ciprofloxacin-resistant methicillin-resistance Staphylococcus aureus. *Bioorganic Chem.* **2020**, *103*, 104231. [CrossRef] [PubMed]
23. Ghafelehbashi, R.; Akbarzadeh, I.; Yaraki, M.T.; Lajevardi, A.; Fatemizadeh, M.; Saremi, L.H. Preparation, physicochemical properties, in vitro evaluation and release behavior of cephalexin-loaded niosomes. *Int. J. Pharm.* **2019**, *569*, 118580. [CrossRef] [PubMed]
24. Mehrarya, M.; Gharehchelou, B.; Poodeh, S.H.; Jamshidifar, E.; Karimifard, S.; Far, B.F.; Akbarzadeh, I.; Seifalian, A. Niosomal formulation for antibacterial applications. *J. Drug Target.* **2022**, *30*, 476–493. [CrossRef] [PubMed]
25. Jain, A.P.; Sharma, P.; Pandey, P.; Gupta, R.; Roshan, S.; Garg, A.; Sahu, A.; Jain, A. Niosome a novel approach for drug delivery system: An overview. *Asian J. Pharm. Sci. Res.* **2013**, *3*, 18–30.
26. Fahmy, S.A.; Sedky, N.K.; Ramzy, A.; Abdelhady, M.M.M.; Alabrahim, O.A.A.; Shamma, S.N.; Azzazy, H.M.E.-S. Green extraction of essential oils from Pistacia lentiscus resins: Encapsulation into Niosomes showed improved preferential cytotoxic and apoptotic effects against breast and ovarian cancer cells. *J. Drug Deliv. Sci. Technol.* **2023**, *87*, 104820. [CrossRef]
27. Bendas, E.R.; Abdullah, H.; El-Komy, M.H.; Kassem, M.A. Hydroxychloroquine niosomes: A new trend in topical management of oral lichen planus. *Int. J. Pharm.* **2013**, *458*, 287–295. [CrossRef]
28. Moghassemi, S.; Hadjizadeh, A. Nano-niosomes as nanoscale drug delivery systems: An illustrated review. *J. Control. Release* **2014**, *185*, 22–36. [CrossRef]
29. Al Jayoush, A.R.; Hassan, H.A.F.M.; Asiri, H.; Jafar, M.; Saeed, R.; Harati, R.; Haider, M. Niosomes for nose-to-brain delivery: A non-invasive versatile carrier system for drug delivery in neurodegenerative diseases. *J. Drug Deliv. Sci. Technol.* **2023**, *89*, 105007. [CrossRef]
30. Canton, R.; Morosini, M.I. Emergence and spread of antibiotic resistance following exposure to antibiotics. *FEMS Microbiol. Rev.* **2011**, *35*, 977–991. [CrossRef]
31. Abonashey, S.G.; Hassan, H.A.F.M.; Shalaby, M.A.; Fouad, A.G.; Mobarez, E.; El-Banna, H.A. Formulation, pharmacokinetics, and antibacterial activity of florfenicol-loaded niosome. *Drug Deliv. Transl. Res.* **2024**, *14*, 1077–1092. [CrossRef] [PubMed]
32. Guinedi, A.S.; Mortada, N.D.; Mansour, S.; Hathout, R.M. Preparation and evaluation of reverse-phase evaporation and multilamellar niosomes as ophthalmic carriers of acetazolamide. *Int. J. Pharm.* **2005**, *306*, 71–82. [CrossRef] [PubMed]
33. El-Ela, F.I.A.; Gamal, A.; Elbanna, H.A.; ElBanna, A.H.; Salem, H.F.; Tulbah, A.S. In Vitro and In Vivo Evaluation of the Effectiveness and Safety of Amygdalin as a Cancer Therapy. *Pharmaceuticals* **2022**, *15*, 1306. [CrossRef] [PubMed]
34. AbuBakr, A.H.; Hassan, H.; Abdalla, A.; Khowessah, O.M.; Abdelbary, G.A. Therapeutic potential of cationic bilosomes in the treatment of carrageenan-induced rat arthritis via fluticasone propionate gel. *Int. J. Pharm.* **2023**, *635*, 122776. [CrossRef]
35. Shaker, D.S.; Shaker, M.A.; Hanafy, M.S. Cellular uptake, cytotoxicity and in-vivo evaluation of Tamoxifen citrate loaded niosomes. *Int. J. Pharm.* **2015**, *493*, 285–294. [CrossRef]
36. Chen, H.C.; Cheng, S.H.; Tsai, Y.H.; Hwang, D.F. Determination of tiamulin residue in pork and chicken by solid phase extraction and HPLC. *J. Food Drug Anal.* **2006**, *14*, 80–83. [CrossRef]
37. Salem, H.F.; Kharshoum, R.M.; El-Ela, F.I.A.; Abdellatif, K.R.A. Evaluation and optimization of pH-responsive niosomes as a carrier for efficient treatment of breast cancer. *Drug Deliv. Transl. Res.* **2018**, *8*, 633–644. [CrossRef]
38. Gamal, A.; Saeed, H.; Sayed, O.M.; Kharshoum, R.M.; Salem, H.F. Proniosomal Microcarriers: Impact of Constituents on the Physicochemical Properties of Proniosomes as a New Approach to Enhance Inhalation Efficiency of Dry Powder Inhalers. *AAPS PharmSciTech* **2020**, *21*, 156. [CrossRef]
39. Yoder, H.W., Jr. A historical account of the diagnosis and characterization of strains of Mycoplasma gallisepticum of low virulence. *Avian. Dis.* **1986**, *30*, 510–518. [CrossRef]
40. Frey, M.L.; Anderson, D.P.; Hanson, R.P. Airsacculitis relation to mycoplasmas in turkeys free of Mycoplasma gallisepticum. *Avian. Dis.* **1968**, *12*, 693–699. [CrossRef]
41. Tanner, A.C.; Wu, C.C. Adaptation of the Sensititre broth microdilution technique to antimicrobial susceptibility testing of Mycoplasma gallisepticum. *Avian. Dis.* **1992**, *36*, 714–717. [CrossRef] [PubMed]

42. Gharaibeh, S.; Hailat, A. Mycoplasma gallisepticum experimental infection and tissue distribution in chickens, sparrows and pigeons. *Avian Pathol* **2011**, *40*, 349–354. [CrossRef] [PubMed]
43. Marouf, S.; Moussa, I.M.; Salem, H.; Sedeik, M.; Elbestawy, A.; Hemeg, H.A.; Dawoud, T.M.; Mubarak, A.S.; Mahmoud, H.; Alsubki, R.A.; et al. A picture of Mycoplasma gallisepticum and Mycoplasma synoviae in poultry in Egypt: Phenotypic and genotypic characterization. *J. King Saud Univ.-Sci.* **2020**, *32*, 2263–2268. [CrossRef]
44. Avakian, A.P.; Kleven, S.H.; Glisson, J.R. Evaluation of the specificity and sensitivity of two commercial enzyme-linked immunosorbent assay kits, the serum plate agglutination test, and the hemagglutination-inhibition test for antibodies formed in response to Mycoplasma gallisepticum. *Avian. Dis.* **1988**, *32*, 262–272. [CrossRef]
45. Amer, M.; Hanafei, A.; El-Bayomi, K.; Zohair, G. Comparative study on the efficacy of some antiMycoplasma drugs on the performance of commercial broiler flocks from infected breeders. *Glob. Vet.* **2009**, *3*, 69–74.
46. Shang, R.; Zhang, C.; Yi, Y.; Liu, Y.; Pu, W. Determination of a New Pleuromutilin Derivative in Broiler Chicken Plasma by RP-HPLC-UV and Its Application to a Pharmacokinetic Study. *J. Chromatogr. Sci.* **2018**, *56*, 604–610. [CrossRef]
47. Elazab, S.T.; Elshater, N.S.; Hashem, Y.H.; Park, S.C.; Hsu, W.H. Tissue Residues and Pharmacokinetic/Pharmacodynamic Modeling of Tiamulin Against Mycoplasma anatis in Ducks. *Front. Vet. Sci.* **2020**, *7*, 603950. [CrossRef]
48. Cao, C.; Liu, Y.; Zhang, G.; Dong, J.; Xu, N.; Zhou, S.; Yang, Y.; Yang, Q.; Ai, X. Temperature-Dependent Residue Depletion Regularities of Tiamulin in Nile Tilapia (*Oreochromis niloticus*) Following Multiple Oral Administrations. *Front. Vet. Sci.* **2021**, *8*, 679657. [CrossRef]
49. Balakrishnan, P.; Shanmugam, S.; Lee, W.S.; Lee, W.M.; Kim, J.O.; Oh, D.H.; Kim, D.-D.; Kim, J.S.; Yoo, B.K.; Choi, H.-G. Formulation and in vitro assessment of minoxidil niosomes for enhanced skin delivery. *Int. J. Pharm.* **2009**, *377*, 1–8. [CrossRef]
50. Chen, S.; Hanning, S.; Falconer, J.; Locke, M.; Wen, J. Recent advances in non-ionic surfactant vesicles (niosomes): Fabrication, characterization, pharmaceutical and cosmetic applications. *Eur. J. Pharm. Biopharm.* **2019**, *144*, 18–39. [CrossRef]
51. Kumar, G.P.; Rajeshwarrao, P. Nonionic surfactant vesicular systems for effective drug delivery—An overview. *Acta Pharm. Sin. B* **2011**, *1*, 208–219. [CrossRef]
52. Hao, Y.; Zhao, F.; Li, N.; Yang, Y.; Li, K.A. Studies on a high encapsulation of colchicine by a niosome system. *Int. J. Pharm.* **2002**, *244*, 73–80. [CrossRef] [PubMed]
53. Bernsdorff, C.; Wolf, A.; Winter, R.; Gratton, E. Effect of hydrostatic pressure on water penetration and rotational dynamics in phospholipid-cholesterol bilayers. *Biophys. J.* **1997**, *72*, 1264. [CrossRef] [PubMed]
54. El-Laithy, H.M.; Shoukry, O.; Mahran, L.G. Novel sugar esters proniosomes for transdermal delivery of vinpocetine: Preclinical and clinical studies. *Eur. J. Pharm. Biopharm.* **2011**, *77*, 43–55. [CrossRef]
55. Kirby, C.; Clarke, J.; Gregoriadis, G. Effect of the cholesterol content of small unilamellar liposomes on their stability in vivo and in vitro. *Biochem. J.* **1980**, *186*, 591–598. [CrossRef]
56. Biswal, S.; Murthy, P.; Sahu, J.; Sahoo, P.; Amir, F. Vesicles of non-ionic surfactants (niosomes) and drug delivery potential. *Int. J. Pharm. Sci. Nanotechnol.* **2008**, *1*, 1–8. [CrossRef]
57. Nasseri, B. Effect of cholesterol and temperature on the elastic properties of niosomal membranes. *Int. J. Pharm.* **2005**, *300*, 95–101. [CrossRef]
58. Nasseri, B.; Florence, A.T. Microtubules formed by capillary extrusion and fusion of surfactant vesicles. *Int. J. Pharm.* **2003**, *266*, 91–98. [CrossRef]
59. Marın, M.T.; Margarit, M.V.; Salcedo, G.E. Characterization and solubility study of solid dispersions of flunarizine and polyvinylpyrrolidone. *Il Farm.* **2002**, *57*, 723–727. [CrossRef]
60. Mohsen, A.M.; AbouSamra, M.M.; ElShebiney, S.A. Enhanced oral bioavailability and sustained delivery of glimepiride via niosomal encapsulation: In-vitro characterization and in-vivo evaluation. *Drug Dev. Ind. Pharm.* **2017**, *43*, 1254–1264. [CrossRef]
61. Sezgin-Bayindir, Z.; Onay-Besikci, A.; Vural, N.; Yuksel, N. Niosomes encapsulating paclitaxel for oral bioavailability enhancement: Preparation, characterization, pharmacokinetics and biodistribution. *J. Microencapsul.* **2013**, *30*, 796–804. [CrossRef] [PubMed]
62. Yaghoobian, M.; Haeri, A.; Bolourchian, N.; Shahhosseni, S.; Dadashzadeh, S. The Impact of Surfactant Composition and Surface Charge of Niosomes on the Oral Absorption of Repaglinide as a BCS II Model Drug. *Int. J. Nanomed.* **2020**, *15*, 8767–8781. [CrossRef] [PubMed]
63. Rege, B.D.; Kao, J.P.; Polli, J.E. Effects of nonionic surfactants on membrane transporters in Caco-2 cell monolayers. *Eur. J. Pharm. Sci.* **2002**, *16*, 237–246. [CrossRef] [PubMed]
64. Colorado, D.; Fernandez, M.; Orozco, J.; Lopera, Y.; Muñoz, D.L.; Acín, S.; Balcazar, N. Metabolic Activity of Anthocyanin Extracts Loaded into Non-ionic Niosomes in Diet-Induced Obese Mice. *Pharm. Res.* **2020**, *37*, 152. [CrossRef]
65. Manasa, R.; Shivananjappa, M. Role of Nanotechnology-Based Materials in Drug Delivery. In *Advances in Novel Formulations for Drug Delivery*; Wiley: Hoboken, NJ, USA, 2023; pp. 279–307.
66. Arzani, G.; Haeri, A.; Daeihamed, M.; Bakhtiari-Kaboutaraki, H.; Dadashzadeh, S. Niosomal carriers enhance oral bioavailability of carvedilol: Effects of bile salt-enriched vesicles and carrier surface charge. *Int. J. Nanomed.* **2015**, *10*, 4797–4813.
67. Zhang, Y.; Gan, Y.; Wang, J.; Feng, Z.; Zhong, Z.; Bao, H.; Xiong, Q.; Wang, R. Dysbiosis of Gut Microbiota and Intestinal Barrier Dysfunction in Pigs with Pulmonary Inflammation Induced by Mycoplasma hyorhinis Infection. *mSystems* **2022**, *7*, e0028222. [CrossRef]

68. Sun, F.; Yang, S.; Zhang, H.; Zhou, J.; Li, Y.; Zhang, J.; Jin, Y.; Wang, Z.; Li, Y.; Shen, J.; et al. Comprehensive Analysis of Tiamulin Metabolites in Various Species of Farm Animals Using Ultra-High-Performance Liquid Chromatography Coupled to Quadrupole/Time-of-Flight. *J. Agric. Food Chem.* **2017**, *65*, 199–207. [CrossRef]
69. Sun, F.; Zhang, H.; Gonzales, G.B.; Zhou, J.; Li, Y.; Zhang, J.; Jin, Y.; Wang, Z.; Li, Y.; Cao, X.; et al. Unraveling the Metabolic Routes of Retapamulin: Insights into Drug Development of Pleuromutilins. *Antimicrob. Agents Chemother.* **2018**, *62*, e02388-17. [CrossRef]
70. Murayama, A.; Abukawa, D.; Watanabe, K.; Umebayashi, H.; Inagaki, T.; Miura, K.; Takeyama, J. Severe liver dysfunction in patients with Mycoplasma pneumoniae infection. *Pediatr. Int.* **2010**, *52*, e105–e107. [CrossRef]
71. Poddighe, D. Mycoplasma pneumoniae-related hepatitis in children. *Microb. Pathog.* **2020**, *139*, 103863. [CrossRef]
72. Feitosa, R.C.; Geraldes, D.C.; Beraldo-de-Araujo, V.L.; Costa, J.S.R.; Oliveira-Nascimento, L. Pharmacokinetic Aspects of Nanoparticle-in-Matrix Drug Delivery Systems for Oral/Buccal Delivery. *Front. Pharmacol.* **2019**, *10*, 1057. [CrossRef] [PubMed]